

Mass mapping of a new area of neutron-deficient sub-uranium nuclides

June 11, 2001

Yu.N. Novikov^{a,b}, F. Attallah^a, F. Bosch^a, M. Falch^c, H. Geissel^{a,d}, M. Hausmann^a, Th. Kerscher^c, O. Klepper^a, H.-J. Kluge^a, C. Kozhuharov^a, Yu.A. Litvinov^{a,b,1}, K.E.G. Löbner^c, G. Münzenberg^{a,e}, Z. Patyk^f, T. Radon^a, C. Scheidenberger^a, A.H. Wapstra^g, H. Wollnik^d

^a *Gesellschaft für Schwerionenforschung, Planckstrasse 1, D-64291 Darmstadt, Germany*

^b *St. Petersburg Nuclear Physics Institute, Gatchina 188350 and St. Petersburg State University, 198904, Russia*

^c *Sektion Physik, Ludwig-Maximilians-Universität München, Am Coulombwall, D-85748 Garching, Germany*

^d *II. Physikalisches Institut, Universität Giessen, Heinrich-Buff-Ring 16, D-35392 Giessen, Germany*

^e *Johannes Gutenberg Universität, Staudingerweg 7, D-55099 Mainz, Germany*

^f *Soltan Institute for Nuclear Studies, PL-00681, Warsaw, Poland*

^g *National Institute of Nuclear Physics and High Energy Physics, NIKHEF, PO Box 41882, 1009DB Amsterdam, The Netherlands*

Abstract

The masses of 64 short-lived neutron-deficient nuclides covering the element range from tungsten to uranium have been obtained for the first time. They have been evaluated by combining directly measured masses from Schottky Mass Spectrometry with linked experimental Q-values in α -decay chains. Based on these new mass data we have determined the one-proton and two-proton drip-lines as well as the size of the “littoral shallow” of the sea of instability. No evidence of a Thomas-Ehrman shift has been found in the region of the investigated heavy nuclides. A peculiar behavior of two-proton separation energies has been observed in the lead region. The predictive power of various mass models is investigated.

PACS: 21.10.Dr, 27.70.+q, 27.80.+w, 29.20.Dh, 29.30.Aj

¹Corresponding author. Tel.: +49-6159-71-2142; fax: +49-6159-71-2902; e-mail: Y.Litvinov@gsi.de.

Introduction

Recent direct mass-measurements [1] at GSI have covered the bottom part of the neutron-deficient unknown mass surface in the sub-bismuth region of the chart of nuclides. The masses of 104 nuclides with half-lives longer than 10 s have been measured for the first time. The technique of Schottky Mass Spectrometry (SMS), which is based on the detection of the revolution frequencies of highly-charged ions stored and electron cooled in the storage ring ESR [2, 3], was used at the SIS-FRS-ESR facility. The results obtained in ref. [1] covered an area that had been chosen because it includes nuclides at the onset of α -radioactivity, which belong to the endpoints of known α -decay chains. The starting points of these long chains are very short-lived nuclides far off β -stability. Their masses have been unknown and presently they cannot be measured directly via SMS because of their short half-lives. However, the combination of directly measured masses of [1] with α -spectroscopy data allows one to determine the masses of these nuclides and, hence, to extend the measured mass-surface considerably to the exotic region of nuclides beyond the proton drip-line. Based on the new mass data, which can be obtained in this way and from the data of [1], a variety of important topics is discussed.

1. The mass information for a new area of the chart of nuclides provides a challenging test for existing mass formulae and allows an examination of their predictive power.
2. The mass data allow to determine the proton drip-line in this mass region.
3. This also opens the possibility to determine nuclei that can undergo proton decay. An estimation of the proton radioactivity region becomes possible.
4. For even-even nuclides a more reliable prediction of the position of the two-proton drip-line can be given.
5. The existence of a Thomas-Ehrman shift in heavy nuclides can be tested.
6. The mass-mapping of exotic nuclides in this region allows to study the strength of the $Z=82$ shell closure for nuclides far from β -stability.

1 New masses obtained with α -decay chains

The neutron-deficient side of heavy nuclides starting from mass numbers $A \approx 150$ contains a region of α -emitters. These α -emitters are linked by numerous decay chains, each containing from 3 to 6 nuclides in the sub-uranium region. Some of the nuclides situated at the ends of the α -chains have half-lives longer than 10 s. This is the typical minimum time necessary for SMS with exotic nuclei. The masses of these long-lived members of the α -chains have been measured directly by SMS [1].

If the atomic mass value for one nuclide (Z, A) in an α -decay chain is known, then the mass value of the i -th member of the chain can be written as:

$$M(Z + 2i, A + 4i)c^2 = M(Z, A)c^2 + \sum_{k=1}^i Q_{\alpha_k} + iM(^4He)c^2. \quad (1)$$

Here Q_{α_k} is the energy of the k -th transition in the chain which is equal to $Q_{\alpha_k} = E_{\alpha_k} \cdot A_k / (A_k - 4)$ where E_{α_k} is the kinetic energy of the corresponding α -particles. In cases where excited states in either the mother or daughter nucleus are involved the corresponding excitation energies have been taken into account. These values are zero for even-even nuclides, but can be larger for odd-odd and odd-A nuclides [4].

The used Q_α -values for ground-to-ground state transitions are given in Table 1. These values have been evaluated from known measured data updated in 2000 [5]. Table 1 lists the resulting mass values for ground states of nuclides which are linked by α -decay chains. Mass values in atomic units are shown in column 6 of Table 1. The corresponding uncertainties are given in column 7. The values for the mass excess (M - A) and their uncertainties are presented in columns 8 and 9, respectively.

In case of chains of odd-A or odd-odd nuclides we have chosen as a starting point for the mass evaluation those nuclides which have no known isomeric states and which masses have been measured directly. The masses for all the members of these chains could then be unambiguously assigned. However, there are α -chains for which the directly measured mass values can contain a mixture of both ground and isomeric states. For some cases the measured value can unambiguously be assigned to ground or isomeric states [1]. The other cases, where the isomeric state contribution is not known, and the mass evaluation of nuclides within the α -chains had to be based on them are marked by an asterisk in column 10 of Table 1. In addition, the excitation energy (in keV) of the corresponding isomeric state of the nuclide, given in parentheses, is presented in column 10. This value can be considered as upper limit for an additional systematic uncertainty of the mass value. Tentative values (two asterisks) have been assigned to nuclides belonging to an α -decay chain starting at the nuclide ^{200}Fr whose decay scheme is not yet firmly established. The masses based on the nuclides which were remeasured in ref. [1] with an uncertainty improving the published values of 150 keV or higher (see ref. [6],[7]) are marked by the label “*r*” in Table 1.

The mass values given in column 6 of Table 1 are rounded-off values obtained by using not-rounded directly measured mass values [1] and Q_α data of column 4. The error bars for the mass values (columns 7 and 9 of Table 1) were obtained from the uncertainties of the Q_α -values and of the directly measured mass values.

Table 1. Mass values derived in this work for the ground states of nuclides linked by α -decay chains. The index "r" represents remeasured mass value, * marks unfavored cases followed by the excitation energies of the corresponding isomeric states, in keV, and ** - tentative values.

El	A	$T_{1/2}$	Q_α (μu)	σ_{Q_α} (μu)	Mass (u)	σ_M (μu)	M - A (keV)	$\sigma_{(M-A)}$ (keV)	Comments
W	168	53 s	4838	13	167.951820	110	-44880	100	
Os	172	19 s	5610	6	171.960030	110	-37230	100	
Pt	176	6.3 s	6319	3	175.968950	110	-28920	100	
Hg	180	2.6 s	6718	4	179.978270	120	-20240	110	
Hg	182	10.8 s	6438	5	181.974740	110	-23530	100	
Hg	183	8.8 s	6483	4	182.974380	110	-23860	100	
Tl	185	19.5 s	6107	54	184.978680	120	-19860	110	
Pb	184	0.55 s	7272	4	183.988150	120	-11040	110	
Pb	186	4.8 s	6947	6	185.984290	110	-14630	100	
Pb	187	15 s	6867	8	186.983850	110	-15040	100	
Bi	189	0.68 s	7802	4	188.989080	120	-10170	110	
Bi	190	6.3 s	7367	5	189.988470	190	-10740	180	
Bi	191	12 s	7279	3	190.985760	100	-13260	90	
Po	188	≈ 0.4 ms	8682	27	187.999430	120	-530	110	
Po	190	2.4 ms	8262	7	189.995160	110	-4510	100	
Po	191	22 ms	8039	9	190.994490	110	-5130	100	
Po	192	38 ms	7858	8	191.991390	110	-8020	100	
Po	193	0.36 s	7615	4	192.991030	100	-8360	90	
Po	194	0.39 s	7503	3	193.988160	100	-11030	90	r
Po	195	4.6 s	7243	3	194.988080	110	-11100	100	* $\approx 90(^{191}\text{Pb})$
Po	196	5.8 s	7146	3	195.985470	100	-13530	90	
At	193	34 ms	8041	6	192.999730	120	-250	110	
At	194	0.28 s	7881	6	193.998960	190	-970	180	
At	195	0.4 s	7880	5	194.996240	100	-3500	90	
At	196		7548	16	195.995440	120	-4250	110	**
At	197	0.39 s	7624	3	196.993240	110	-6300	100	
At	198	4.2 s	7400	3	197.992970	100	-6550	90	* $\approx 270(^{194}\text{Bi})$
At	199	7.2 s	7278	3	198.990560	100	-8790	90	
At	200	43 s	7081	2	199.990520	100	-8830	90	* 270 (^{196}Bi)
At	201	89 s	6949	2	200.988460	100	-10750	90	r
At	202	3 min	6829	2	201.988660	100	-10560	90	* $\approx 150(^{198}\text{Bi})_r$
Rn	195	≈ 6 ms	8260	12	195.005350	110	4980	100	
Rn	196	4.4 ms	8177	10	196.002170	110	2020	100	
Rn	197	65 ms	7955	8	197.001590	100	1480	90	
Rn	198	64 ms	7890	4	197.998660	100	-1250	90	r
Rn	199	0.62 s	7656	6	198.998340	110	-1550	100	* $\approx 90(^{191}\text{Pb})$
Rn	200	1.06 s	7562	3	199.995630	100	-4070	90	
Rn	201	7 s	7365	2	200.995650	120	-4050	110	* $\approx 230(^{197}\text{Po})$
Rn	202	9.85 s	7272	2	201.993270	100	-6270	90	
Rn	203	45 s	7117	3	202.993640	100	-5920	90	* 312(^{199}Po)
Rn	204	1.2 min	7027	2	203.991460	100	-7950	90	
Rn	205	2.8 min	6856	2	204.991920	100	-7530	90	* 424(^{201}Po)

El	A	$T_{1/2}$	Q_α (μu)	σ_{Q_α} (μu)	Mass (u)	σ_M (μu)	M - A (keV)	$\sigma_{(M-A)}$ (keV)	Comments
Rn	206	5.7 min	6853	2	205.990180	100	-9150	90	
Fr	200		8271	16	200.006310	120	5880	110	**
Fr	201	69 ms	8068	7	201.003910	110	3640	100	
Fr	202	≈ 0.3 s	7932	6	202.003500	100	3260	90	* $\approx 270(^{194}\text{Bi})$
Fr	203	0.55 s	7812	5	203.000980	100	910	90	
Fr	204	1.5 s	7699	3	204.000820	100	760	90	* $270(^{196}\text{Bi})$
Fr	205	3.8 s	7573	3	204.998640	100	-1270	90	r
Fr	206	16 s	7436	5	205.998700	100	-1210	90	* $\approx 150(^{198}\text{Bi}),\text{r}$
Ra	202	0.7 ms	8609	66	202.009870	120	9190	110	
Ra	203	≈ 1 ms	8298	22	203.009240	110	8610	100	* $\approx 90(^{191}\text{Pb})$
Ra	204	59 ms	8197	9	204.006430	100	5990	90	
Ra	205	0.21 s	8037	22	205.006290	120	5860	110	* $\approx 230(^{197}\text{Po})$
Ra	206	0.24 s	7960	5	206.003830	100	3570	90	
Ra	207	1.3 s	7808	3	207.004060	100	3780	90	* $312(^{199}\text{Po})$
Ra	208	1.3 s	7808	5	208.001870	100	1740	90	
Ra	209	4.6 s	7672	5	209.002200	100	2050	90	* $424(^{201}\text{Po})$
Ra	210	3.7 s	7682	5	210.000470	100	440	90	
Ac	206	≈ 22 ms	8528	32	206.014630	110	13630	100	* $\approx 270(^{194}\text{Bi})$
Ac	207	≈ 27 ms	8421	27	207.012000	110	11180	100	
Ac	208	95 ms	8295	15	208.011720	100	10920	90	* $270(^{196}\text{Bi})$
Ac	209	91 ms	8302	10	209.009540	100	8890	90	r
Ac	210	0.35 s	8166	9	210.009470	100	8820	90	* $\approx 150(^{198}\text{Bi}),\text{r}$
Th	209	≈ 4 ms	8843	76	209.017740	150	16520	140	* $\approx 230(^{197}\text{Po})$
Th	210	9 ms	8645	18	210.015080	100	14050	90	
Th	211	37 ms	8527	15	211.015190	110	14150	100	* $312(^{199}\text{Po})$
Th	212	30 ms	8537	11	212.013010	100	12120	90	
Th	213	0.14 s	8415	8	213.013220	100	12310	90	* $424(^{201}\text{Po})$
Th	214	0.1 s	8399	8	214.011470	100	10680	90	
Pa	212	≈ 5 ms	9049	60	212.023370	120	21770	110	* $270(^{196}\text{Bi})$
Pa	213	≈ 5.3 ms	9011	21	213.021160	110	19710	100	r
Pa	214	17 ms	8879	21	214.020950	110	19510	100	* $\approx 150(^{198}\text{Bi}),\text{r}$
U	218	1.5 ms	9432	21	218.023510	110	21900	100	

2 Predictive power of various mass models

A large number of mass models have been proposed and developed over the last decades. They are based on different assumptions and belong either to pure microscopic models, which start from the nucleon-nucleon interaction, to macroscopic-microscopic approaches, which use a modified liquid-drop model with shell and pairing corrections, to shell model mass predictions focused on narrow regions in the nuclear chart or to special mass relations combining masses of adjacent nuclides.

Critical assessments of nuclear mass models have been done in ref.[8] -[11]. The most crucial test of the reliability of mass models are new experimental data in the regions of

nuclides where masses had been unknown when the model was formulated.

To obtain the rms-deviation σ_{rms} of a model we have used the expression [12]

$$\sigma_{rms}^2 = \frac{1}{n} \sum_{i=1}^n (M_{exp} - M_{th})_i^2, \quad (2)$$

where M_{exp} and M_{th} denote the experimental and theoretical mass values, respectively.

Table 2. Predictive power of various mass models: (a) presents the rms-deviations for the set of 194 mass values from this work and ref.[1], (b) shows the rms-deviations for the complete set of previously experimentally known masses taken from ref.[6]

Mass Formula	Model	σ_{rms} (keV) (a)	σ_{rms} (keV) (b)
Goriely [13]	Thomas-Fermi	646	732
Myers-Swiatecki [14]	Thomas-Fermi	417	698
Tondeur et al.[15]	Hartree-Fock	852	718
Duflo-Zucker[16]	microscopic approach	654	580
Möller-Nix[12]	macro- microscopic	431	827
Möller et al.[12]	finite-range droplet and folded-Yukawa potential	407	678
Spanier-Johansson [12]	liquid drop with corrections	1195	743
Satpathy-Nayak [12]	infinite nuclear matter	1112	691
Tachibana et al. [12]	empirical p-n interaction	718	547
Masson-Jänecke [12]	equation with isospin contributions	593	327
Jänecke-Masson [12]	mass relations	488	263
Comay-Kelson [12]	mass relations	532	350
Audi-Wapstra et al.[6]	extrapolations from experi- mentally known masses	138	-

The rms-deviations for some tabulated mass model predictions [17] as well as for the empirical extrapolations [6] are presented in Table 2.

The rms-deviations for the set of 194 mass values presented in this work and in ref.[1] are shown in column 3 (labeled (a)). As can be seen from this column none of the tested models predicts the new experimental data with an accuracy of better than 400 keV. Only the extrapolations of [6] are satisfactory.

For comparison we present in Table 2 the rms-deviations for the complete set of previously experimentally known masses [6] (labeled (b)). Comparing the two rms-values for the different models, one finds that the majority of the models fits better to the previously

known masses (to which they have been partly adjusted) than to the new mass data. This shows that the predictive power of these models is rather poor, at least in the region studied here. Only the models which use Thomas-Fermi calculations (Goriely et al. and Myers-Swiatecki) and the macro-microscopic approach (Möller-Nix and Möller et al.) show a better predictive power.

3 One-proton and two-proton drip-lines

One of the exciting applications of the derived mass-surface is the possibility to identify the proton drip-line in the region of the chart of nuclides with $75 \leq Z \leq 91$.

Important work on this subject has been done in investigations on proton radioactivity of some of the isotopes in the region $Z \leq 83$ [18]-[25].

We used the equation

$$S_p(Z, N) = B(Z, N) - B(Z - 1, N) = (M(Z - 1, N) + M(1, 0) - M(Z, N))c^2 \quad (3)$$

to determine the pair of nuclides $(Z - 1, N)$ and (Z, N) for which the proton separation energy S_p changes sign. Here B and M stand for the total binding energies and the atomic mass values of the nuclides, respectively.

Fig.1 shows the values of one-proton separation energies obtained in this work for ground states of odd- Z isotopes.

As can be seen from this figure the position of the one-proton drip-line can definitely be identified for the region $83 \leq Z \leq 91$. For other Z -values we give interpolated results.

To determine the two-proton drip-line we used the expression

$$S_{2p} = B(Z, N) - B(Z - 2, N) = (M(Z - 2, N) + 2M(1, 0) - M(Z, N))c^2. \quad (4)$$

We have determined the values of the two-proton separation-energy S_{2p} for even-even nuclides and show them as a function of the mass number A in Fig. 2. One can use linear extrapolations of the behaviour of S_{2p} to zero to predict the two-proton drip-line. As seen from Fig. 2 the position of this line on the chart of nuclides can now be located in the region $74 \leq Z \leq 88$ and especially for mercury, lead and polonium isotopes.

Fig.3 presents a part of the chart of nuclides in the sub-uranium region. The nuclides for which the mass values were determined for the first time are shown by grey squares. The positions of one- and two-proton drip-lines determined from experimental mass-data are shown. The known proton emitters are also indicated. We like to emphasize that the determination of the S_p -values and hence the border line is based only on the unambiguous data in Table 1. The S_{2p} - values were derived from the masses of even-even nuclides, which are definitely ground states.

The knowledge of the position of one- and two-proton drip-lines is important for the systematic search for proton radioactivity. Roughly the region of proton radioactivity can be defined for nuclides with half-lives longer than 10^{-12} s, the approximate limit for the definition of radioactivity as such [26]. Then one can approximately determine the proton decay energy $Q_p = -S_p$, which corresponds to this half-life limit and, using the extrapolation of the S_p -data of Fig.1, the respective nuclei.

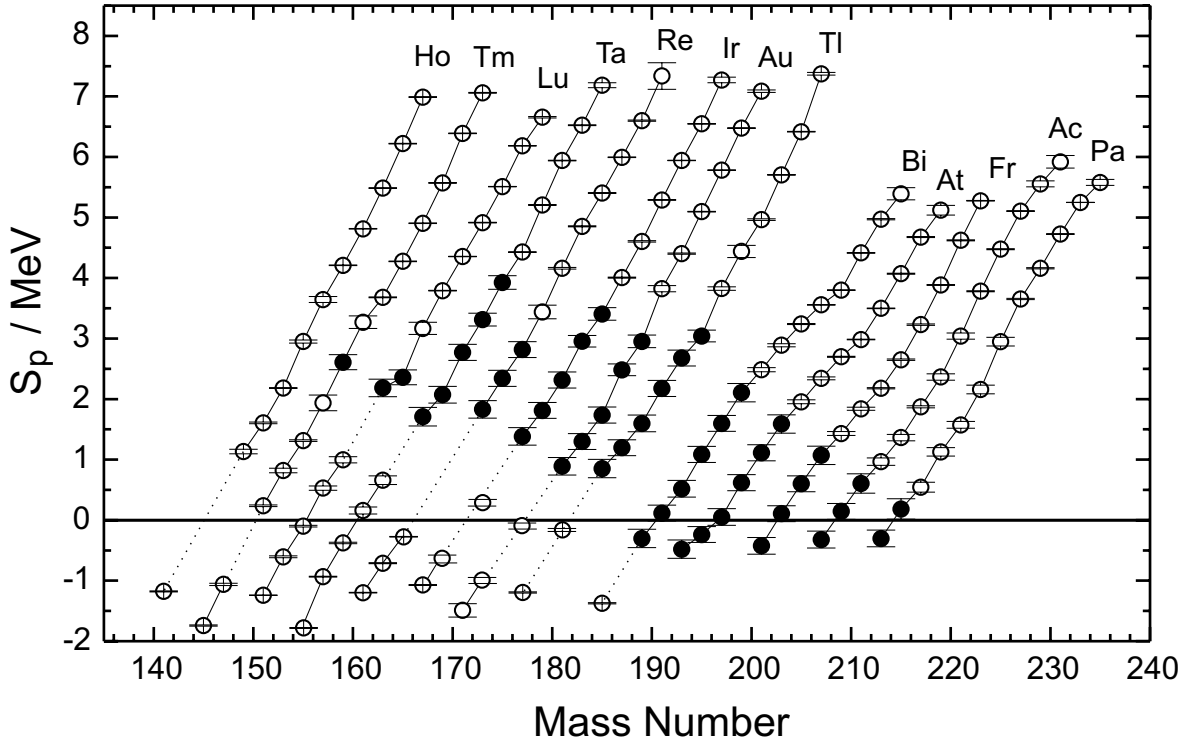


Figure 1: One-proton separation energies for odd- A and odd- Z isotopes of the elements from Ho to Pa obtained in this work (full circles) and taken from [7] (open circles). The proton decay energies for ground states of proton unstable nuclides (open circles for negative S_p values) are taken from the refs.[18]-[25].

Spectroscopic information in this region of interest is extremely limited. Most of the nuclides have not been observed at all. Therefore, we used a simple approximation for the barrier penetration by protons which provides a satisfactory connection of Q_p and $T_{1/2}$ (see, e.g., [26]). We used for our extrapolations a very rough dependence of S_p on A in the form $S_p = a + b \cdot A^{-1/3} + c \cdot A^{-1}$, which is based on the liquid-drop model. Extrapolated curves have been obtained by fitting only a restricted number of positive S_p -values closest to the proton drip-line. In this way, we avoid uncertainties from neglecting higher order terms in the formula used for S_p .

Fig.4 shows the size of the region of proton radioactivity, which might be called “littoral shallow” of the sea of instability. The position of the outer border of this “shallow” depends not only on Q_p -values, but also on the orbital angular momenta l_p of protons, which in our estimations we assumed to be zero. For isotopes of some of the elements (Ta, Re, Ir, Au and Tl) whose ground-states have spin value $1/2^+$ (see Fig.4) this is a reasonable assumption. For other elements the spin values of the nuclides are higher which can increase the half-lives and therefore will move the border away from the proton drip-line. The border shown in Fig.4 reflects the minimal size of the region of proton radioactivity.

For light and medium mass nuclides the “littoral shallow” should be smaller due to the

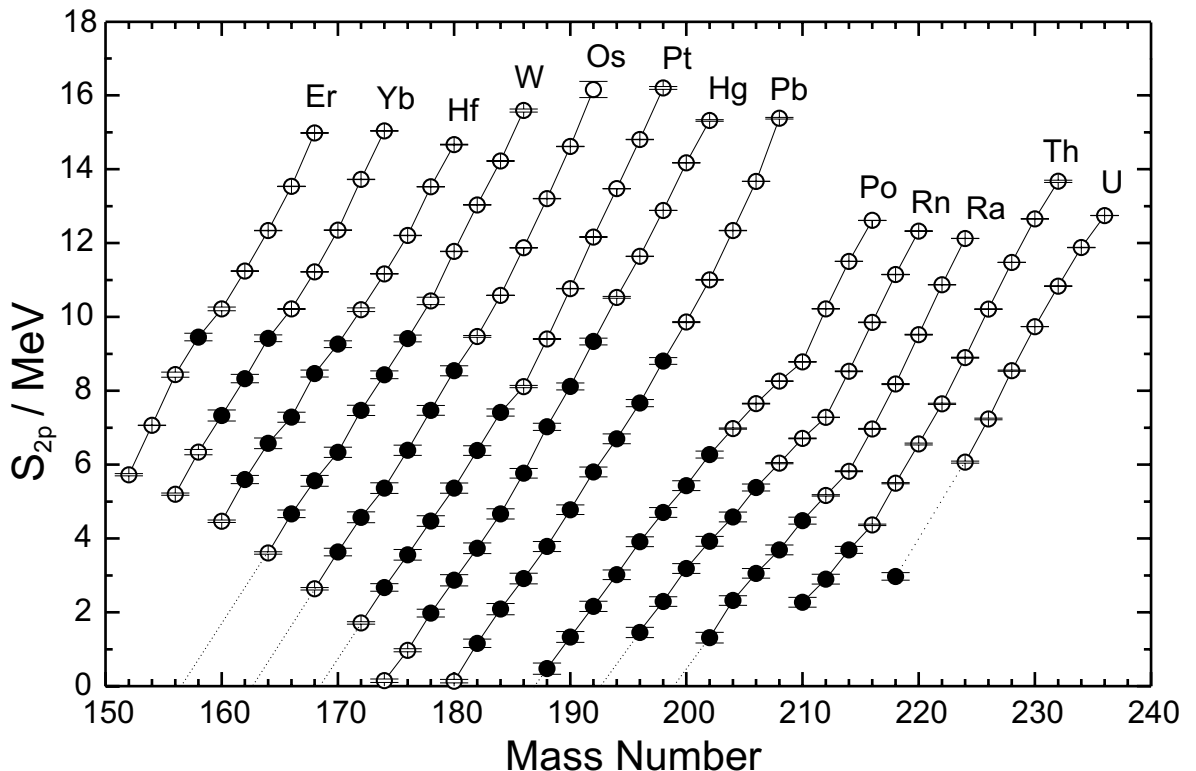


Figure 2: Two-proton separation energies for even-even isotopes of the elements from Er to U obtained in this work (full circles) and taken from ref.[7] (open circles). The dotted lines have been used for extrapolations or interpolations. The values for ^{174}Hg and ^{180}Pb have been evaluated by using the recent results of refs.[27, 28] and of ref.[7]

lower Coulomb barrier which gives smaller Q_p -values for $T_{1/2} \simeq 10^{-12} s$.

4 On the problem of the Thomas-Ehrman shift in heavy nuclides

Our predictions of the position of the borders of the “littoral shallow” could be changed if a considerable shift of the proton separation energy would exist due to the so called Thomas-Ehrman (T.-E.) effect [29, 30]. The same changes due to the Coulomb correlations [31] should be expected for the proton drip-line. The knowledge of the position of the proton drip-line on the other hand is important for predictions of the path of rapid proton capture process in stellar nucleosynthesis. Since the position of the proton drip-line is still unknown for nuclides with $Z \geq 39$, there are uncertainties in the rp-path for sub-tin nuclides [32]. Thus, the existence (or nonexistence) of a T.-E. shift in medium and heavy nuclides is crucial. Since this effect has been observed in the very light mirror nuclides (^{13}C - ^{13}N) as a relative shift of unbound analog states equal to $\simeq 700$ keV, one might conclude that this phenomenon is a privilege of light nuclides (see also ref.[33]).

This effect was explained as a reduction of Coulomb energy for proton-unbound states

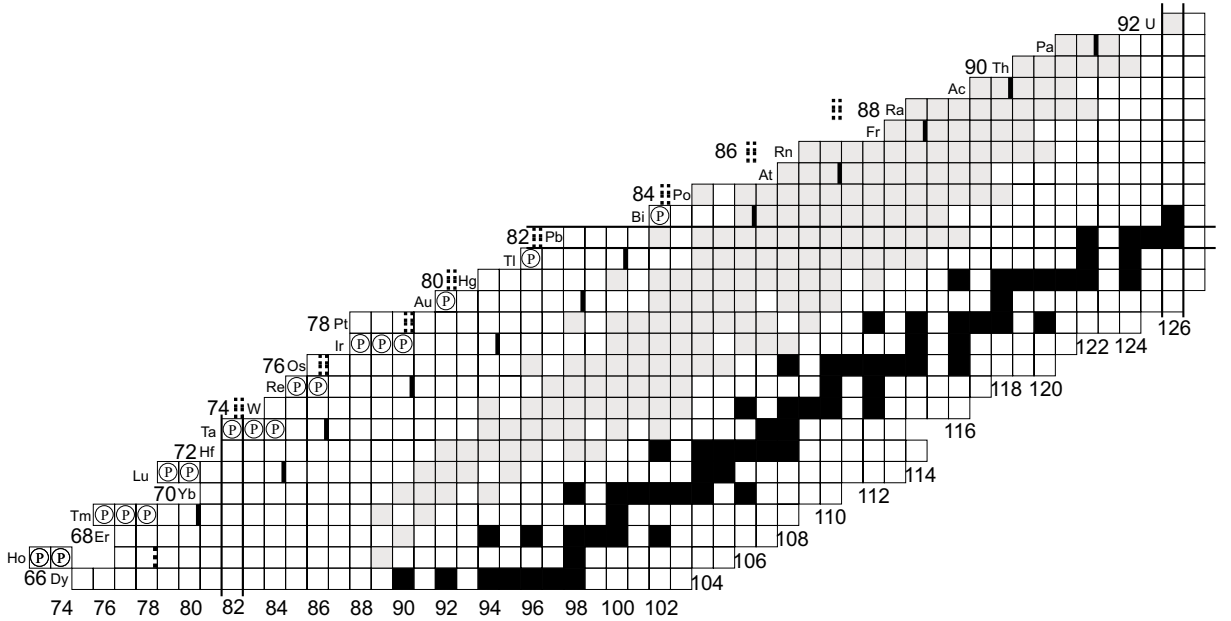


Figure 3: Part of the Chart of Nuclides. The nuclides whose masses are determined for the first time (or remeasured with better precision) [1] and evaluated in this work using α -decay chains are shown by grey squares. One- and two-proton drip-lines identified on the basis of experimental data obtained in this work are shown by single and by double vertical lines, respectively (dashed lines indicate the extrapolated or interpolated data). Known proton emitters are indicated by circles containing the letter “P”.

where the single particle wave function is pushed out of the nuclear interior. As the Coulomb barrier, which confines the wave function inside the nuclear interior, is small in light nuclides and the centrifugal barrier is usually small as well, it was thought that the shift should be significant in light nuclear systems. This conclusion was supported by S-matrix calculations [34] which gave the estimation of the upper limit of the shift in terms of the width of the level.

The possibility to identify the T.-E. shift in the region of the proton drip-line in light and medium mass nuclides was formulated in [35]. These authors obtained on the average for proton-unbound nuclides a large difference of -576 keV between experimental and calculated mass values with a particular mass relationship [36]. On the other hand, the average difference for proton-bound nuclei was with 3.4 keV surprisingly small. Thus, an unambiguous manifestation of the T.-E. shift both in magnitude and in sign was claimed. A rather large difference of -234 ± 50 keV was determined for the medium-weight nuclide ^{39}Sc which has a small proton decay energy of about 450 keV and a high spin-value of $7/2^-$. Both characteristics would favor a small shift [37].

Recently [38, 39] a significant T.-E. shift was predicted for other medium-weight nuclides close to the proton drip-line.

The existence of the T.-E. shift could be seen in our data as a kink in the smooth behavior of the proton separation energies crossing the A-axis ($S_p=0$). If it exists, the bound proton ground states for odd-Z nuclides are shifted towards the proton-rich side.

The new mass information allows to perform this analysis. One needs to know S_p for

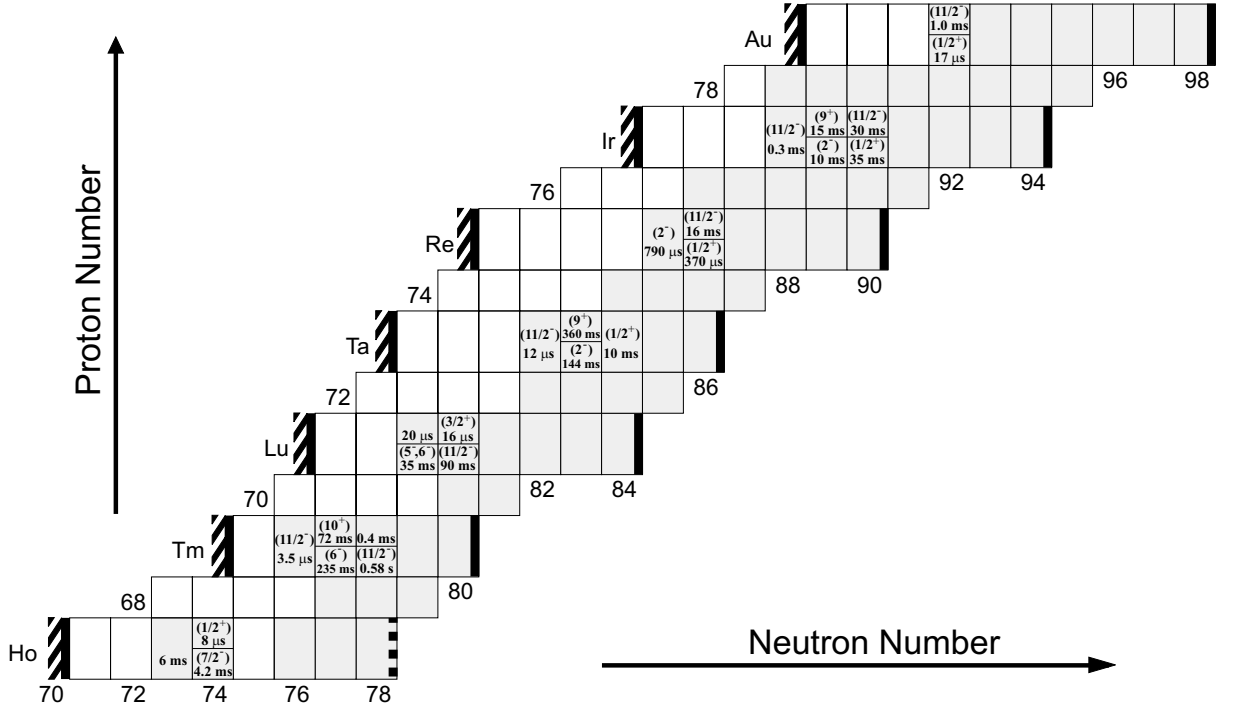


Figure 4: “Littoral shallow” on a part of the chart of nuclides. The proton drip-line is shown for odd- Z elements by vertical lines, whereas the outer border corresponding to $T_{1/2} = 10^{-12}$ s and $l_p = 0$ by bold lines with hatching. The known nuclides are given by grey squares. The spin and half-life values for known proton emitters are shown as well.

proton-unbound nuclides and for a group of proton-bound isotopes close to the drip line. The odd- A proton-unbound isotopes of the elements Ta, Re, Ir, Bi^m and At have spin values equal to $1/2^+$. This strongly favors [37] a T.-E. shift because of the small angular momentum and the high value of the principal quantum number.

The procedure of extrapolation has been described already in section 3. The fitted curves are presented in Fig.5. This figure shows that the fit procedure is quite satisfactory for all presented cases. The average value for the shifts of S_p from the extrapolated curves for all proton unbound nuclides turned out to equal (-20 ± 60) keV. Thus, we can conclude that there is no evidence for the existence of a Thomas-Ehrman shift in heavy nuclei.

5 Peculiar behavior of two-proton separation energies in the lead region

The experimental information about masses obtained in this work allows to determine the behavior of two-proton separation energies for nuclides far from the β -stability line. We can define

$$2G_p(Z, N) \equiv S_{2p}(Z, N) - S_{2p}(Z+2, N) = (M(Z-2, N) - 2M(Z, N) + M(Z+2, N))c^2. \quad (5)$$

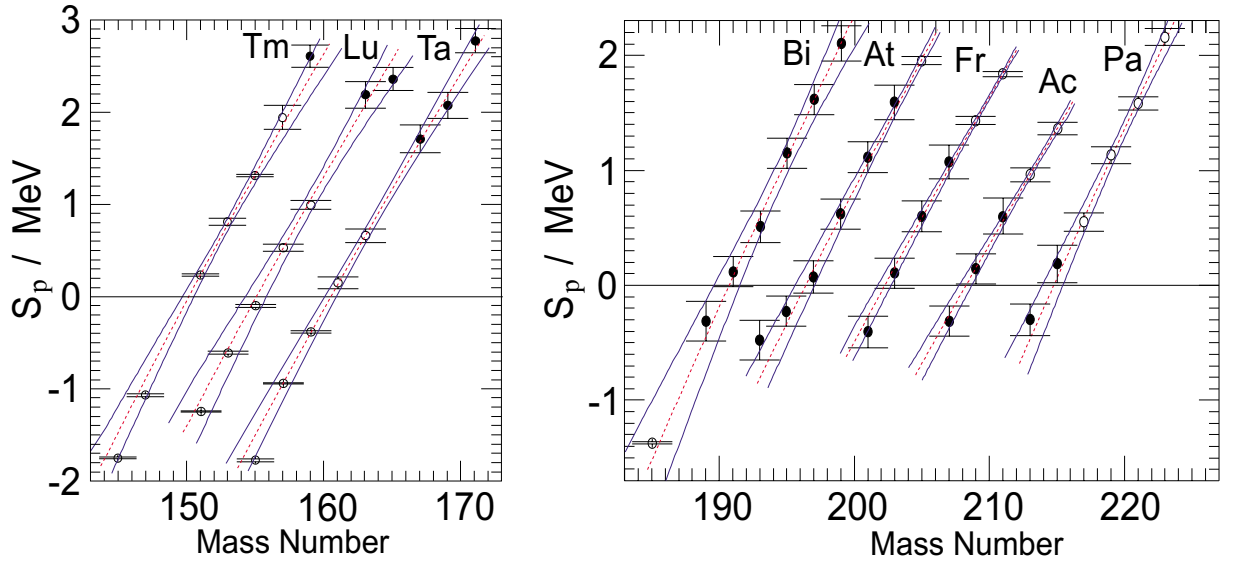


Figure 5: Fit of the proton separation-energies by polynomial function (dashed, see text). Only the points with positive S_p -values have been used for this procedure. The values obtained in this work have been marked by full circles. The solid lines indicate the range of uncertainties.

For magic nuclides the quantity G_p is related to the single particle shell gap. Changing the N-values for various Z-numbers (Z and N even), we can see how the value G_p behaves moving away from N=126. The values of $2G_p$ derived from the Table 1 and ref. [1] are presented in Fig.6. One can see from this figure that the value of $2G_p$ reaches ~ 7 MeV for the doubly magic nuclide ^{208}Pb due to the “mutual support” of two magic numbers [40]. However, it becomes much smaller in the region of N=106 ($2G_p \simeq 2.5$ MeV), which is 20 neutrons away from the magic number N=126.

The reasons for this strong decrease of G_p towards the proton drip-line could be changes in the shape of nuclides, changes in correlation energies or a lowering of the energies of single particle intruder states [41].

A different trend can be observed for nuclides with other nucleon magic numbers. Indeed, Fig.7 shows the behavior of the G_p gap for Z=50 nuclides close and far from stability and Figs.8 and 9 show the behavior of the G_n gaps around N=82 and N=126, correspondingly. The data for these figures have been taken from ref.[7].

The G -values for Z=50 and N=82 nuclides remain big also far from the β -stability line, whereas there is not enough information for N=126 nuclides. At least, within the known mass region there is no indication yet for a strong quenching of the G_n for N=126 nuclides. Thus, the G_p quenching phenomenon illustrated above for Z=82 nuclides is a peculiar feature of this Z-value.

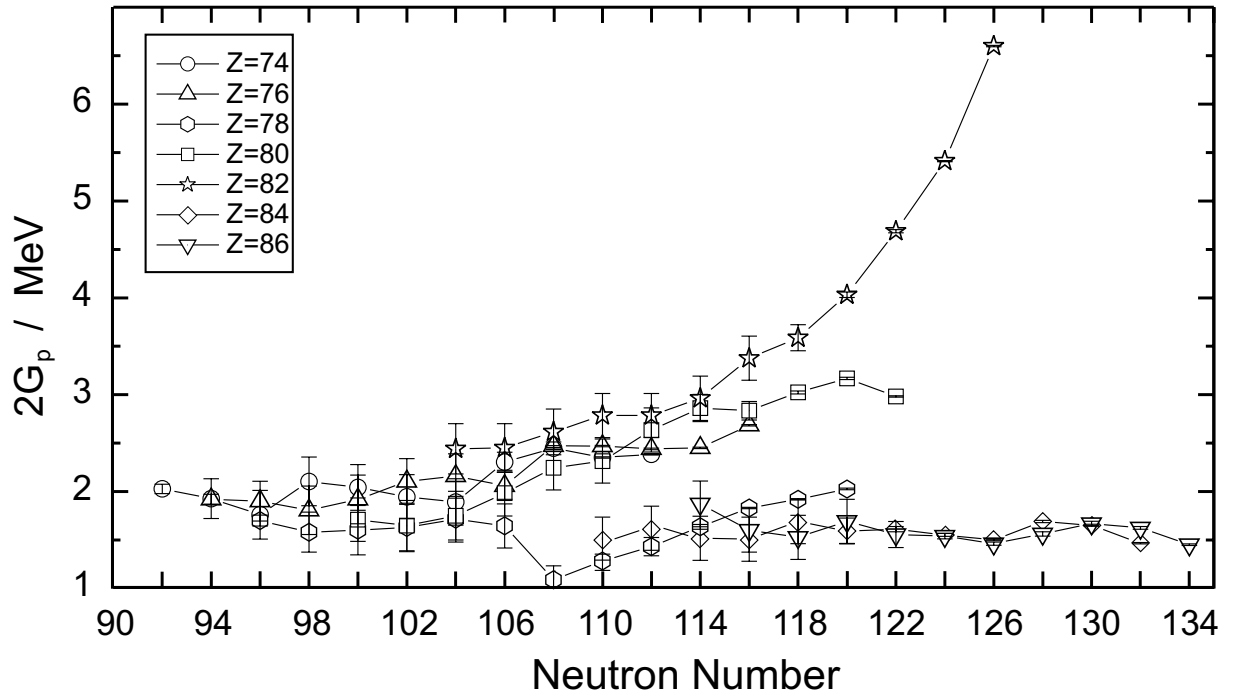


Figure 6: Differences between the two-proton separation energies $S_{2p}(Z, N) - S_{2p}(Z+2, N)$ for different Z -values in the vicinity of $Z=82$ as a function of N .

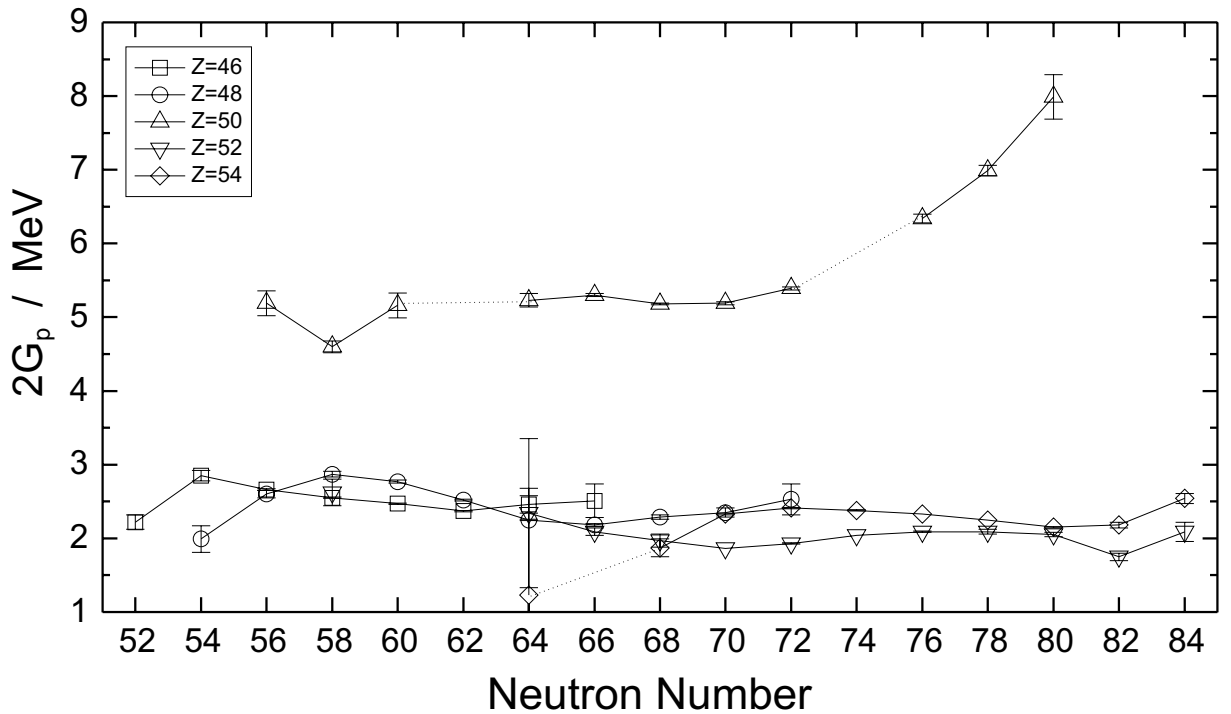


Figure 7: Differences between the two-proton separation energies for different Z -values in the vicinity of $Z=50$ as a function of N .

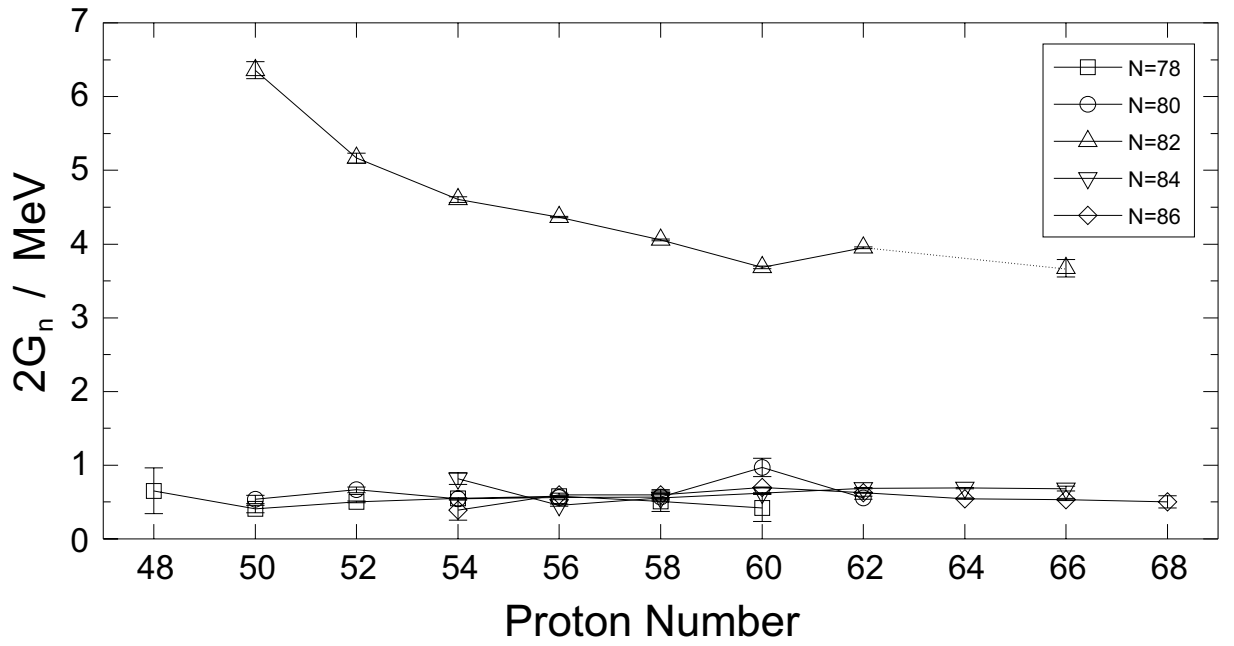


Figure 8: Differences between the two-neutron separation energies $S_{2n}(Z, N) - S_{2n}(Z, N+2)$ for different N-values in the vicinity of N=82 as a function of Z.

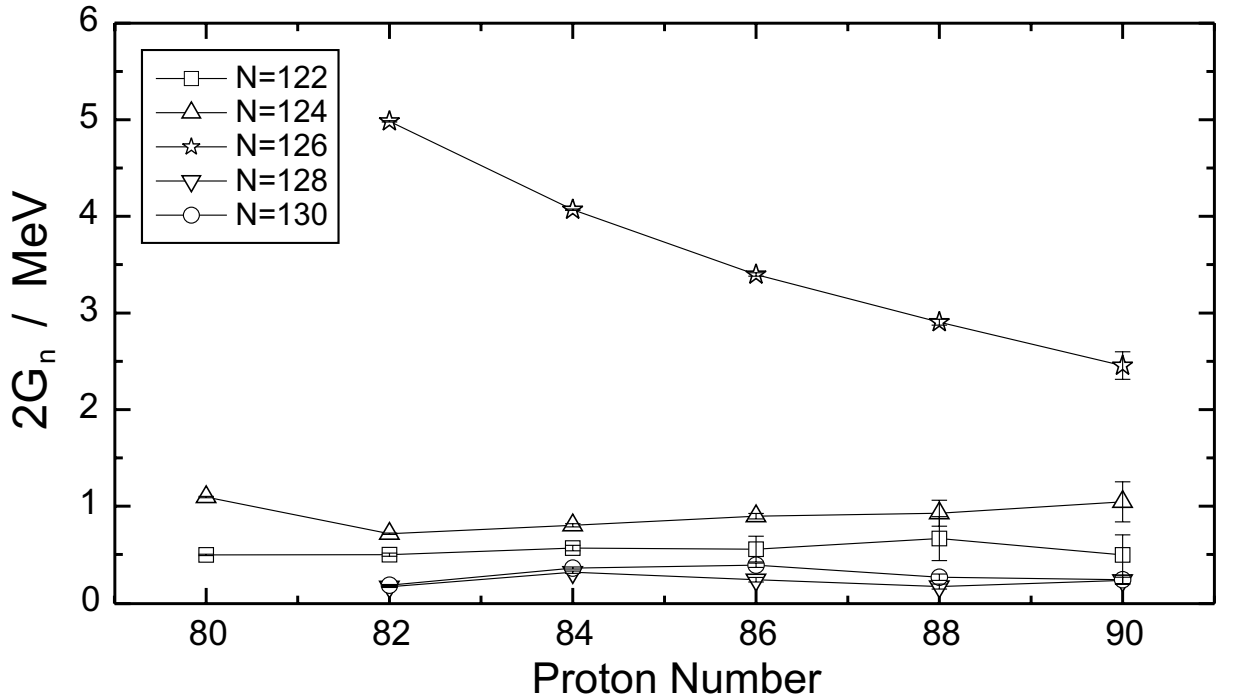


Figure 9: Differences between the two-neutron separation energies for different N-values in the vicinity of N=126 as a function of Z.

6 Conclusion

Mass values within α -decay chains derived in this work in addition to the direct mass measurements [1] performed at the SIS-FRS-ESR facility at GSI considerably extended the region of known masses. In total, mass values for 168 neutron-deficient nuclides in the region $57 \leq Z \leq 92$ have been obtained for the first time, 64 of which in the region $74 \leq Z \leq 92$ have been obtained in this work. The masses evaluated in this work mostly belong to nuclides on the edge of the nuclear chart.

The presented information gives new insight into the physics of exotic nuclides.

A part of the mapped surface belongs to the area of proton-instability. The proton drip-line has been determined based on our experimental data. The position of the two-proton drip-line has been obtained by extrapolations. The region of proton-radioactive nuclei between holmium and gold has been outlined. The border of this so called “littoral shallow of the sea of instability” is 6 to 10 neutron numbers away from the proton drip-line for odd- Z nuclides. A considerable part of the nuclides belonging to the short-lived proton-emitters, is still unknown. The knowledge of the size of this particular region of the chart of nuclides is useful in planning and understanding of experiments on proton radioactivity.

The analysis of the experimental data shows that there is no Thomas-Ehrman shift in a wide region of heavy nuclides, which could change the position of the proton drip-line.

One of the exciting problems discussed over the years is the “universality” of the well known magic proton and neutron numbers throughout the chart of nuclides. We observed a washing out of the two-proton separation energy gap for lead isotopes far off the β -stability line.

The predictive power of different theoretical mass formulae has been checked for the new mass-surface using 12 different mass models. The result of this comparison shows that neither of the mass formula yields values with an accuracy of better than ~ 0.4 MeV. The extrapolations of Audi-Wapstra [6] satisfactorily agree with our experimental values.

The combination of direct mass measurements and α -spectroscopy data performed in this work allowed to map a wide range of α -emitters. This approach will be extended in our future experiments.

Acknowledgements

The authors would like to thank G. Audi, M. Bender, T. Enqvist, H. Kettunen, M. Leino, J.A. Maruhn, P. Ring, H. Schatz, V. Shaginyan, A. Sobiczewski, J. Stadlmann and W. Swiatecki for fruitful discussions. This work has been financially supported by BMBF under Contract No. 06 GI 4751 and No. 06 LM 363, and the Beschleunigerlaboratorium München. Yu. L. and Yu. N. would like to thank GSI and the II. Physics Institute of the Giessen University for warm hospitality as well as the WTZ fund for financial support under grant No. RUS-654-96. Z.P. would like to acknowledge the GSI for warm hospitality and the Polish Committee for Scientific Research (KBN) for support under grant No. 2P03B 117 15.

References

- [1] T. Radon *et al.*, Nucl. Phys. **A677** (2000) 75.
- [2] B. Franzke *et al.*, Physica Scripta **T59** (1995) 176.
- [3] B. Schlitt *et al.*, Hyp. Int. **99** (1996) 117.
- [4] G. Audi and A.H. Wapstra, Proc.ENAM -95 Conf. Edition Frontiers, p.13 (1995).
- [5] A.H. Wapstra (2000), unpublished.
- [6] G. Audi and A.H. Wapstra, Nucl. Phys. **A595** (1995) 409.
- [7] G. Audi *et al.*, Nucl. Phys. **A624** (1997) 1.
- [8] P.E. Haustein, Proc. AMCO-7 Conf., Darmstadt, p.413 (1984).
- [9] C. Borcea and G. Audi, CSNSM-report 92 (1992) 38.
- [10] P.Möller and J.R. Nix, Inst.of Phys.Conf., series No.132 (1993) 43.
- [11] Z. Patyk *et al.*, Phys. Rev. **C59** (1999) 704.
- [12] P.E. Haustein, Atom Data Nucl. Data Tables **39** (1988) 185.
- [13] S. Goriely, <http://www-astro.ulb.ac.be>.
- [14] W.D. Myers and W.J. Swiatecki, LBL-36803, 1994.
- [15] F. Tondeur *et al.*, Phys. Rev. **C62** (2000) 024308 and <http://www-astro.ulb.ac.be>.
- [16] J. Duflo and A.P. Zuker, Phys. Rev. **C52** (1995) R23 and <http://www-CSNSM.in2p3.fr>.
- [17] *The Isotopes Project Home Page/Atomic masses*, <http://ie.lbl.gov/toimass.html>.
- [18] J. Baltchelder *et al.*, Phys. Rev. **C57** (1998) R1042.
- [19] R. Irvine *et al.*, Phys. Rev. **C55** (1997) R1621.
- [20] C.Davids *et al.*, Phys. Rev. Lett. **76** (1996) 592.
- [21] C. Davids *et al.*, Phys. Rev. **C55** (1997) 2255.
- [22] C. Davids *et al.*, Phys. Rev. Lett. **80** (1998) 1849.
- [23] J. Uusitalo *et al.*, Phys. Rev. **C59** (1999) R2975.
- [24] G. Poli *et al.*, Phys. Rev. **C59** (1999) R2979.
- [25] K. Rykaczewski *et al.*, Phys. Rev. **C60** (1999) 011301-1.
- [26] V.I. Goldanskii, Ann. Rev. Nucl. Sci. **16** (1960) 1.
- [27] J. Uusitalo *et al.*, Z. Phys. **A358** (1997) 375.

- [28] C.R. Bingham *et al.*, Proc. AIP-Conf.(Feb.97), **392(1)** (1997) 341.
- [29] J.B. Ehrman, Phys. Rev. **81** (1951) 412.
- [30] R.G. Thomas, Phys. Rev. **88** (1952) 1109.
- [31] A. Bulgac and V.R. Shaginyan, Eur. Phys. J. **A5** (1999) 247 and Phys. Lett. **B469** (1999) 1.
- [32] H. Schatz *et al.*, Phys. Rep. **294** (1998) 167.
- [33] O. Bohr and B. Mottelson, *Nuclear Structure*, Benjamin, N.Y., 1969, **v.1**.
- [34] H. Weidenmüller, Nucl. Phys. **69** (1965) 113.
- [35] E. Comay *et al.*, Phys. Lett. **210B** (1988) 31.
- [36] G.T. Garvey *et al.*, Rev. Mod. Phys. **41** (1969) S41.
- [37] S. Shlomo, Rep. Prog. Phys. **41** (1978) 957.
- [38] W. Nazarewicz *et al.*, Phys. Rev. **C53** (1996) 740.
- [39] W.E. Ormand, Phys. Rev. **C55** (1997) 2407.
- [40] K.-H. Schmidt and D. Vermeulen, Proc. AMCO-6 Conf., ed by J. Nolen,Jr and W. Benenson. N.Y,-L., p.119 (1979).
- [41] R.A. Sorensen, Nucl. Phys. **A420** (1984) 221.